Article

Use of Satellite SAR for Understanding Long-Term Human Occupation Dynamics in the Monsoonal Semi-Arid Plains of North Gujarat, India

Francesc C. Conesa [1,2,*], **Núria Devanthéry** [3], **Andrea L. Balbo** [1,2], **Marco Madella** [1,2,4,5] **and Oriol Monserrat** [3]

[1] CaSEs-Complexity and Socio-Ecological Dynamics Research Group

[2] Spanish National Research Council (IMF-CSIC), c/ Egipcíaques, 15, Barcelona 08001, Catalonia, Spain; E-mail: balbo@imf.csic.es

[3] Geomatics Division, Catalan Telecommunications Technology Centre (CTTC), Av. Carl Friedrich Gauss, 11, Parc Mediterrani de la Tecnologia, Castelldefels E-08860, Catalonia, Spain; E-mails: nuria.devanthery@cttc.cat (N.D.); oriol.monserrat@cttc.cat (O.M.)

[4] Department of Humanities, Universitat Pompeu Fabra, C/ Ramon Trias Fargas, 25–27, Barcelona 08005, Catalonia, Spain; E-mail: marco.madella@icrea.cat

[5] ICREA-Institució Catalana de Recerca i Estudis Avançats

* Author to whom correspondence should be addressed; E-mail: francesc.cecilia@imf.csic.es; Tel.: +39-442-65-76; Fax: +39-443-00-71.

Abstract: This work explores the spatial distribution of monsoonal flooded areas using ENVISAT C-band Advanced Synthetic Aperture Radar (ASAR) in the semi-arid region of N. Gujarat, India. The amplitude component of SAR Single Look Complex (SLC) images has been used to estimate the extent of surface and near-surface water dynamics using the mean amplitude (MA) of monsoonal (July to September) and post-monsoonal (October to January) seasons. The integration of SAR-derived maps (seasonal flooding maps and seasonal MA change) with archaeological data has provided new insights to understand present-day landscape dynamics affecting archaeological preservation and visibility. Furthermore, preliminary results suggest a good correlation between Mid-Holocene settlement patterns and the distribution and extension of seasonal floodable areas within river basin areas, opening interesting inroads to study

settlement distribution and resource availability in past socio-ecological systems in semi-arid areas.
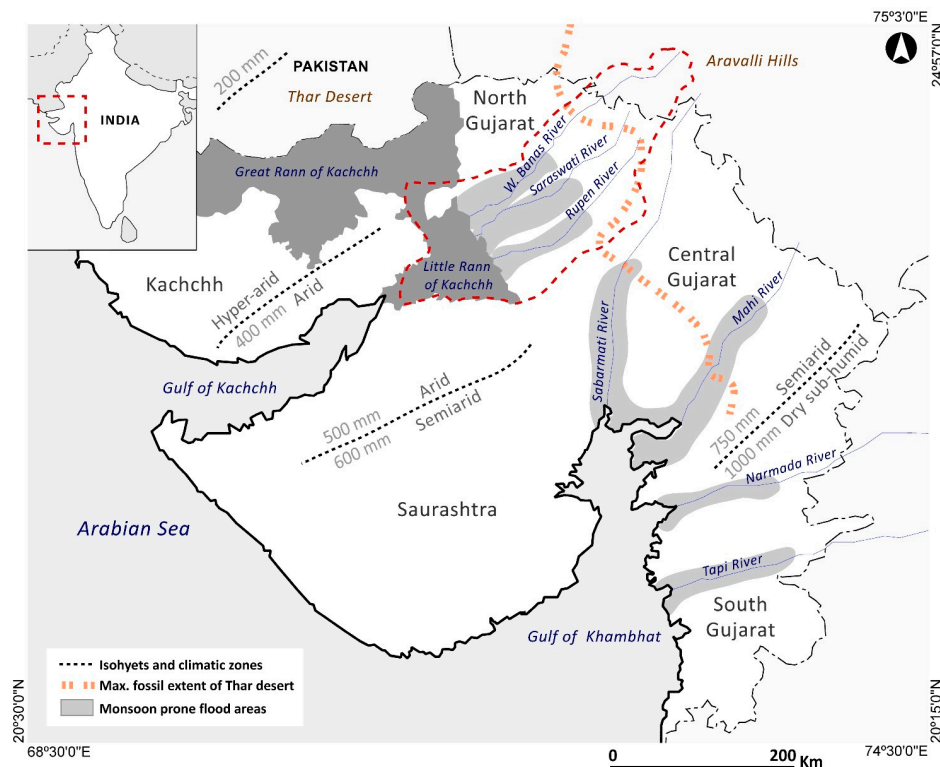
1. Introduction

The understanding of past socio-ecological dynamics emerging in diverse ecological regions has been of particular importance for archaeologists working in South Asia [1–5]. Special attention has been given to regional and local-scale strategies to manage inundation and rain-fed cultivation, accounting for the diversity of landform and inter-annual rainfall variability in the Greater Indus Valley [6,7]. One of the driest regions of India, N. Gujarat is a well-studied peripheral area of the Indus Valley Civilization, being very sensitive to changes in the Indian Summer Monsoon (ISM) precipitation patterns. In these settings, even slight precipitation shifts can generate severe droughts or floods, thus affecting the availability of water and ultimately human adaptive capacity [8–10]. Throughout the Holocene this territory was characterized by desert retreat, the stabilization of dunes and the seasonal presence of water bodies. In this marginal and erratic monsoonal environment, the archaeological evidence suggests the presence of at least three major subsistence systems characterized by different degrees of resilience and adaptability: hunter-gatherers, agro-pastoralists and urban Harappan settlements [11–14]. More than 200 archaeological scatters have been recorded by surveys over the last 20 years [15]. Scatters consist mostly of patches of fragmentary artifacts (lithic, pottery and bone) found on the surface of relict features such as fossilized sand dunes and other non-floodable areas, such as outcrops and islands. To date, archaeological evidence suggests the occupation of these areas as seasonal sites that would take advantage of monsoonal water stored in interdune areas and rich grasslands located in saline or alluvial wastelands [16–18]. Within the framework of the N. Gujarat Archaeological Project (NoGAP, see [19] and [20] for a project overview) and the SimulPast project [21], the use of optical, historical and elevation Earth Observation (EO) data have been explored to support GIS-based landscape investigations [14,22] and modeling socio-ecological dynamics in semi-arid monsoonal environments [23]. Here we use ENVISAT ASAR (Advanced Synthetic Aperture Radar) scenes and optical EO data to evaluate the potential of SAR to better understand the expression of the ISM rainfall in terms of seasonal flooding in the study area and to explore the relationship between seasonal water availability and past settlements patterns.

2. Study Area: Regional Settings and Modern Landscape Dynamics

N. Gujarat extends NE-SW from the foot of the Aravalli Hills to the coast of the Little Rann of Katchchh (LRK), a seasonally flooded marsh along the inner edge of the NW Indian continental platform, situated between the alluvial plains of N. Gujarat and the Kachchh peninsula (Figure 1). The LRK represents the uplifted floor of a former gulf inundated up to c. ~2 ka B.P [24]. To the west, the plains reach the current boundary of the Thar Desert, while the Sabarmati river catchment area and the

Nal Sarovar depression mark its eastern limits [9,25]. The study area integrates three main perennial river basin areas (the West Banas, Saraswati, Rupen and their tributary rivers) that follow the geological slope and drain into the LRK [8,26–28].

Figure 1. Location map of the NoGAP study area (thick dotted red line). Alluvial flood-prone areas are indicated as medium grey shading (after Attri and Tyagi [28], p. 104). Isohyet lines and climatic zones are from Juyal *et al.* [25] (p. 2633), and the maximum fossil extent of Thar Desert is after Singhvi *et al.* [29] (p. 3097).
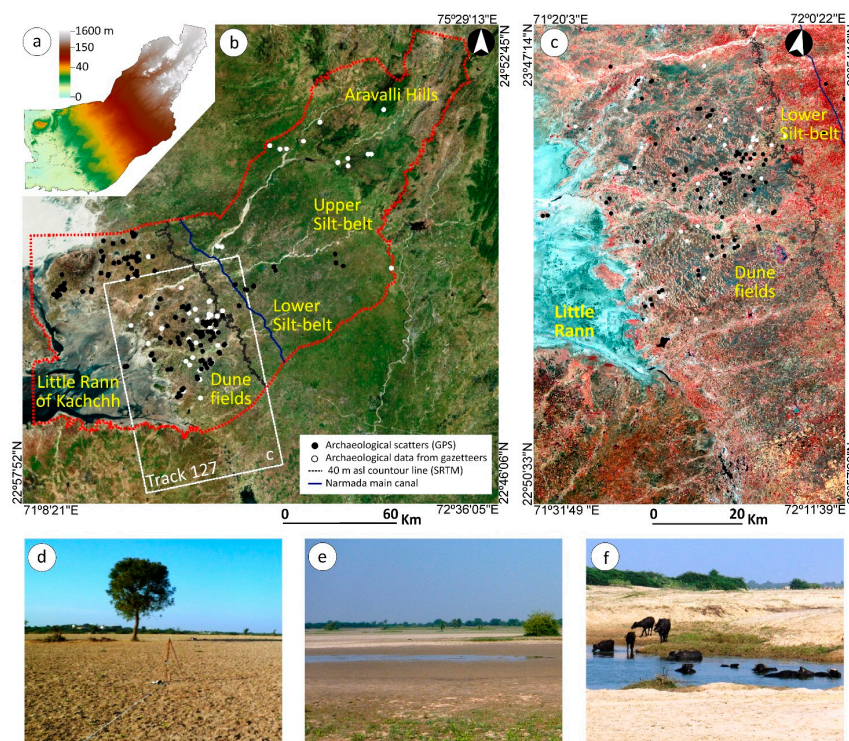

The landscape of N. Gujarat is characterized by the presence of relict sand dunes that were formed c. 26 ka BP [27]. Sedimentary deposits from the Mahi and Sarasbati rivers in Gujarat show a progressive loss of fluvial influence c. 30 ka BP. This suggest that a drier climatic fluctuation affected the area and started deflation processes with Aeolian sediment deposition, thus expanding the active dune belt of the Thar Desert (Figure 1). This arid phase coincides globally with the Last Glacial Maximum (LGM), which fostered the expansion of semi-arid areas in the tropics [29,30]. The more humid Younger Drias (YD) phase c. 12 ka BP restored the monsoon regime [26]. Precipitation anomalies in the ISM were low c. 12–10 ka BP, rising to maximum c. 8 ka BP and lowering until the retiring of the Thar Desert SW boundary to its present position c. 7ka BP, with the consequent stabilization of dunes c. 5 ka BP [31]. Palaeoclimatic records suggest monsoonal stability throughout the mid-Holocene, making this area more suitable for human occupation (see [23] and references therein). Current precipitation patterns indicate a low to moderate ISM characterized by highly erratic and asymmetrical rainfall with strong seasonal variability. The mean annual rainfall values follow a WE trend and vary from 400–800 mm (see isohyet lines in Figure 1). This high temporal and spatial

variability makes N. Gujarat a unique transitional ecosystem between the more humid Indian western coast and the hyper-arid Thar Desert.

The river pools, water tanks and more humid depressions formed patches of grasslands and thorn vegetation that supported considerable large numbers of cattle, goats, water buffaloes as well as wild herbivores and birds [32]. This traditional rain-fed landscape has been gradually transformed for more than four decades, during which the agricultural growth of the region was triggered by the explosion in subsided tube well irrigation, thus bringing more land under cultivation and allowing new rabi irrigated cash-crops and dry-summer crops [33]. Because of the low level of natural recharge of local aquifers, groundwater table has fallen steadily, and soil salinization has become a major problem. These often lead to migration from rural to urban areas [34]. To mitigate the effect of acute water shortages and water table depletion, the Narmada main canal (Nmc) of the Sardar Sarovar Project was recently built across the alluvial plains of N. Gujarat (Figure 2a,b) [35–38].

Figure 2. (**a**) Regional slope (SRTM 90 v4.1, http://srtm.csi.cgiar.org); (**b**) Archaeological scatters within NoGAP research area (red dotted line) and extent of ENVISAT ASAR scenes in ascending mode, Track 127, Swath I6 (base map: ESRI World Imagery); (**c**) Extent of Track 127 displayed as LANDSAT 8 OLI false colour composite (5-4-3, 3 April 2014); (**d**) Fossilized dune surface (Kalrio Timbo archaeological site) during post-monsoon (November 2011; (**e**) Interdune black cotton soils waterlogged during post-monsoon (November 2010); (**f**) West Banas riverbed (November 2011).

The orientation of the canal (SE-NW) is highly influenced by the presence of the West Cambay Basin Margin Fault (WCBMF), a linear disturbance that marks the southern boundary of the rich aquifers located within the tectonic graben (*i.e.*, Cambay Basin) that includes the lower Silt-belt plains (see Figure 2a). The WCBMF boundary coincides with the 40 m a.s.l. (*i.e.*, above sea level) contour

line, and defines a pedagogical and morphological change in the landscape that greatly affects water run-off dynamics and groundwater recharge and affects dune preservation and erosion. The dunes located south of the WCBMF (*i.e.*, dune and interdune fields) are well-preserved dome and linear dunes, while dunes within the lower Silt-belt plains have been highly eroded due to intense mechanized agricultural exploitation with tube-well irrigation. These morphological differences are highly visible in infrared imagery (Figure 2b), where red tones indicate healthy crops and vigorous vegetation in the lower Silt-belt alluvial plains, while bright and dark-green tones indicate sandy dune surfaces and more humid interdune soils respectively (see Balbo *et al.* [14] for further details). On the basis of these premises, the SAR-based landscape observations described in the present work focus on the hydrological dynamics resulting from precipitation discharge, run-off and seasonal concentrations of soil moisture.

3. Materials and Methods

The integration of multi-temporal EO datasets is pivotal for gathering information on landscape and environment variability, including resource spots. However, optical satellite imagery is often limited in monsoonal climates due to the high cloud coverage, the limited access related to on-demand cover and excessive cost for very high resolution data. On the other hand, SAR is an active sensor that emits electromagnetic pulses in the microwave region of the spectrum and collects the electromagnetic waves reflected by the illuminated objects in the direction of the sensor. Medium-resolution satellite SAR imagery has played an important role in tropical and semi-arid contexts due to the capability of microwaves to penetrate clouds, as well as detect soil moisture content in all weather conditions. The detection of soil moisture is key in the study of long-term landscape dynamics as it allows detecting palaeohydrological features, which provide evidence for resource spots important for past human occupation (see [39–43]).

The amplitude of the SAR image is a measure of the backscattered signal of the illuminated objects. The amplitude mainly depends on the roughness and on the dielectric constant of the illuminated target. It is well-established that illuminated rough surfaces provide higher amplitude values, while, in contrast, flat or smooth surfaces reflect most of the signal away from the satellite, thus providing low amplitudes values. Calm water, in particular, returns very low amplitude values compared to rough dry terrain or turbulent open waters. This property makes SAR amplitude images and derived maps very suitable to identify flooded areas and monitor runoff response to spatial variability in precipitation (for examples of flood detection and mapping [44,45].

The full exploitation of SAR imagery for mapping monsoonal floods in NW India remains little explored in spite of the potential of such inexpensive and large-coverage EO products as ERS-1/2 or ENVISAT imagery. SAR imagery has recently been used to monitor hydro-meteorological hazards in the Indus basin, following the 2010 flooding event [46,47] and to address wetland classification and palaeodrainage reconstruction in Rajasthan [48,49]. ERS-1 data has been used to explore flood delineation in the Kutch region of Gujarat [50]. The use of SAR in South Asia is likely to further increase after the completion of the RISAT constellation by the Indian Space Research Organization, with the first Indian-made C-band SAR instrument for civilian use [51]. SAR instruments have found some use in connection with archaeological research in NW South Asia for mapping Harappan
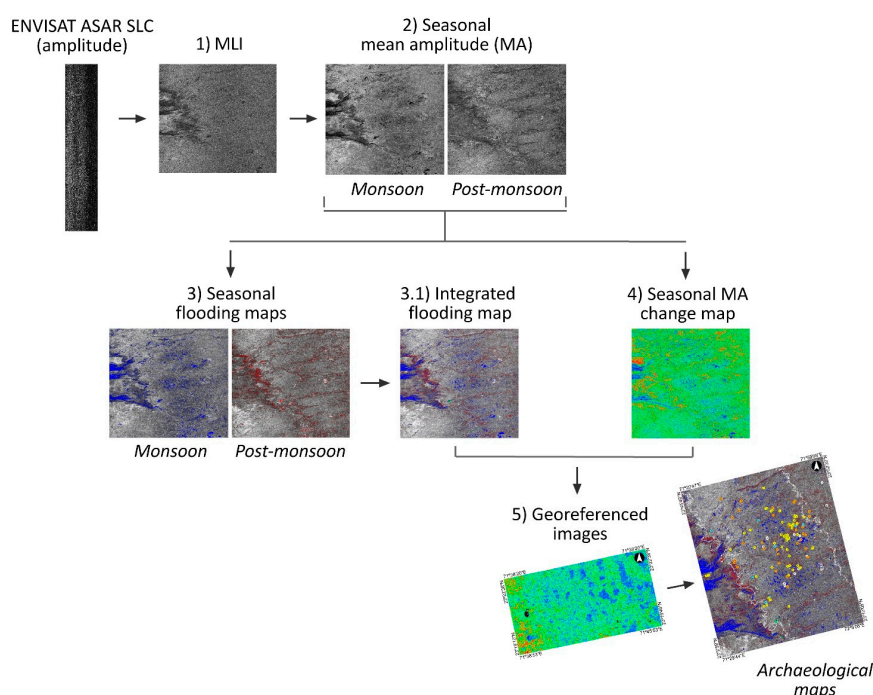
settlements within the Indus and the dried-up Ghaggar-Hakra river basins and tributary palaeochannels ([52–55] and references therein).

3.1. Data Processing

For this study we used five Single Look Complex (SLC) C-band ENVISAT ASAR images, which have a pixel resolution of approximately 20 m × 4 m. The images were acquired in ascending mode (Track 127, see the scene in Figure 2a) acquired between October 2004 and December 2009.
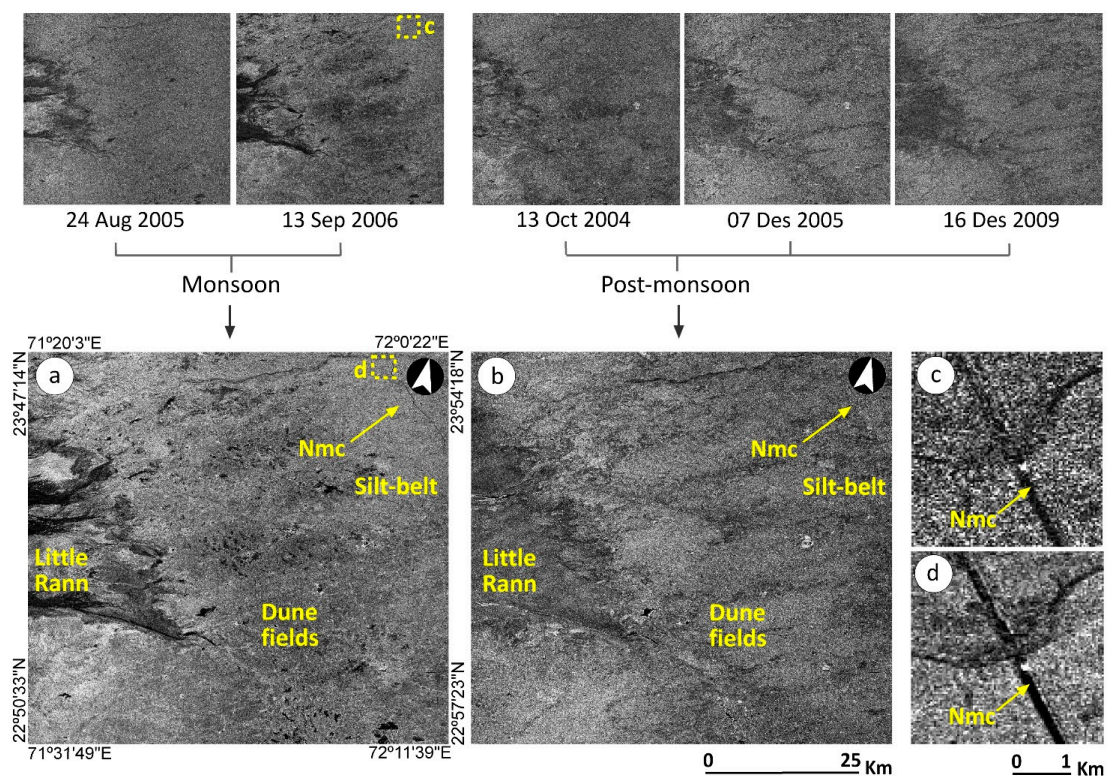
The ASAR scenes were co-registered with respect to a selected master scene and the amplitude image was generated from each scene. The amplitude of each single scene was equalized by dividing the amplitude image by the mean amplitude (MA) value of a subset located in an urban area. The urban area was chosen for the equalization because its measured amplitude has negligible variations during the entire period of study. Through this adjustment, the amplitudes were normalized between the different acquisitions in order to make them comparable. The equalized amplitude is then measured relative to the urban area. In order to reduce the original speckle, a multi-look (MLI) of factor 5 × 1 was performed in each amplitude image. Resulting images were rotated 270° and transposed to geographically orientate the SAR image. Figure 3 sketches the methodological approach, which also builds upon the ENVISAT ASAR amplitude component processing and post-processing chain proposed by Tapete *et al.* [56] and Cigna *et al.* [57].

Figure 3. Workflow employed for the ENVISAT ASAR image processing. After co-registration and equalization, a (**1**) multi-look (MLI) processing was applied to each amplitude scene. (**2**) Images were rotated, transposed, classified upon acquisition time and integrated in two seasonal stacks (MA seasonal images). (**3**) A water threshold was applied to obtain (Section 3.1) seasonal flooding maps. Besides. (**4**) MA images were divided to obtain the seasonal MA change map. (**5**) Final products were georeferenced and integrated into GIS platforms.

Multi-look single amplitude scenes were classified and integrated in two image stacks depending on their date of acquisition (Figure 4). The resulting images represent a seasonal MA scene for both the monsoonal and post-monsoonal season in our study area (Figure 4a,b). In addition, the use of MA images helped to considerably reduce temporal speckle (see the effects of speckle filter in Figure 4c,d).

Figure 4. (**a**) Monsoonal mean amplitude (MA) image generated from two monsoonal scenes; (**b**) Post-monsoonal MA image generated from three monsoonal scenes; (**c**) Detail of radar speckle in ASAR scene (13 September 2006, after MLI processing); (**d**) MA radar speckle reduction (monsoonal MA, after temporal filter).

3.2. Limitations of Using Seasonal MA Scenes

The temporal extent for each seasonal stack was defined after a yearly subdivision of the ISM precipitation patterns suggested as in Balbo *et al*. [23] (Table 1a). The climatic subdivision suggests that within any given year, the ISM generates a strong seasonality that defines three critical moments, each corresponding to a 4-month season. Table 1a shows the average precipitation for each season (mean, median and standard deviation). The Monsoon discharges almost the entire yearly rainfall during summer whereas the post-monsoonal and dry period are characterised by a high variability (note the high standard deviation). These patterns draw attention to the effects of the high inter-annual precipitation variability on the ground. For the period covered in this study (2004–2009), yearly average precipitations (Table 1b) do not exhibit critical events either monthly or annually. Therefore, the observed amplitude values can be used as a representative dataset for the monsoonal and post-monsoonal seasonal average rainfall for our study area. In this study, only the MA response for the monsoonal and post-monsoonal seasons is analysed. As evident from the average data in Table 1b, the major change in rainfall quantity occurs between the monsoon and post-monsoonal period

(a reduction of 80%) whereas the change between post-monsoon and dry period represents a minor change (a decrease of 2%).

Table 1. Climatic subdivision (after Balbo *et al.* [14]) and average seasonal rainfall from Kachchh-Saurashtra region (data from Indian Institute of Tropical Meteorology, http://www.tropmet.res.in).

(a)

Yearly Seasonal Subdivision	Average Precipitation (mm) (1871–2011)		
	Mean	Median	Stdv
June to September (JJAS) Monsoon	1107	1040	492
October to January (ONDJ) Post-monsoon	50	25	61
February to May (FMAM) Dry season	30	11	54

(b)

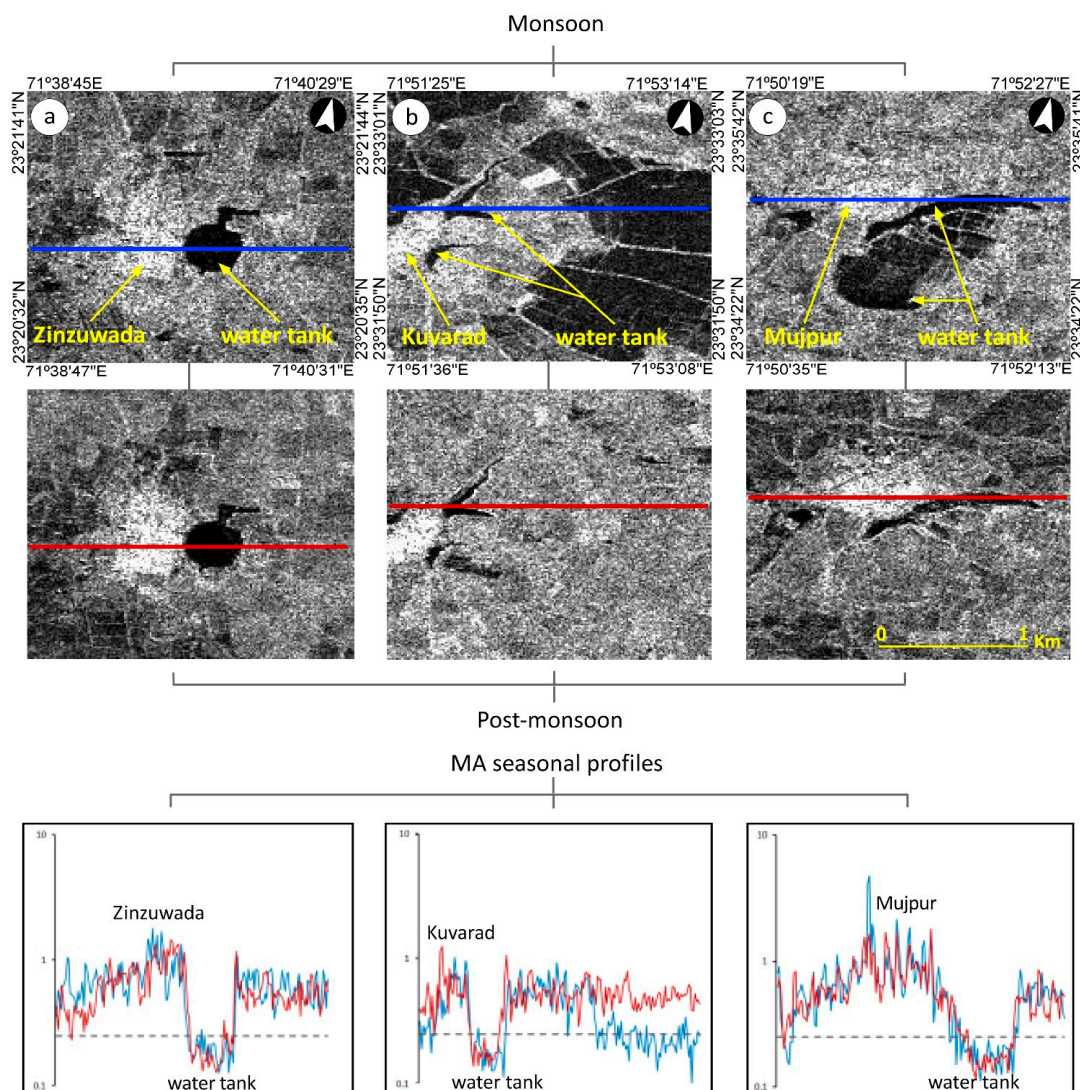| Seasonal Mean Precipitation (mm) for ENVISAT Life Mission (2002–2011)			
ENVISAT Mission Years	Acquired Scenes	Monsoon	Post-Monsoon
2002		850	6
2003		1490	10
2004	13 Oct	984	50
2005	24 Aug; 13 Dec	1426	4
2006	13 Sep	1692	5
2007		2346	7
2008		1379	37
2009	16 Dec	1414	9
2010		2235	116
2011		1641	6

Moreover, the dry season was not integrated in a seasonal stack because only one ascending ENVISAT ASAR scene (acquired in February 2009) was available in the archives, and therefore we could not use mean amplitudes (and reduce the temporal speckle) as for the other periods.

3.3. Empirical MA Threshold for Identification of Flooded Areas

Several authors have applied thresholding methods for the detection of water bodies and to ascertain flooding patterns using the ENVISAT ASAR Global Mode or Wide Swath Mode ([56–59]). The underlying principle of such studies is the lower amplitude produced by calm water surfaces with respect to rougher terrain surfaces. Calm water (as opposite to turbulent water), reflects the incident electromagnetic signal away from the satellite, thus returning a very low amplitude value. Here we exploit this property to extract an empirical MA threshold for identification of flooded areas. The water MA threshold was selected by supervised identification of several types of water bodies in both

periods. In Figure 5, dark and very dark pixels represent a very low amplitude value, which can be related to the presence of water tanks and flooded fields. MA values are extracted from the horizontal profile for both periods. In all cases, the MA corresponding to water bodies was below 0.25 (see bottom row of Figure 5). The applied threshold for surface water was then set to 0.25 for our case of study. Notice that this threshold is valid for the equalization process that was applied to this dataset. Therefore, different equalization would imply different threshold. Water threshold masks were applied to monsoonal and post-monsoonal MA images to generate a new derived image depicting temporal water surface in each seasonal period. The seasonal flooding maps were integrated in a unique map depicting seasonal flooded areas.

Figure 5. Extraction of water threshold values in equalized MA seasonal images from clearly identified water tanks: (**a**) Zinzuwada village; (**b**) Kuvarad village; (**c**) Mujpur village. Image composition shows, in descending order: MA monsoonal image (horizontal blue line); MA post-monsoonal image (horizontal red line); and MA spatial profile (spatially indicated by the horizontal blue and red lines) for monsoonal and post-monsoonal seasons. The water threshold at 0.25 MA value is indicated as a grey dashed line.

3.4. Backscattering Signal Seasonal Change

A seasonal change map was computed by dividing the monsoonal by the post-monsoonal MA values to understand the seasonal reflectivity behaviour within the study area. The resulting MA seasonal change map was classified in three main categories: (a) surface lower reflectivity for the monsoonal period (values from 0 to 1); (b) surface lower reflectivity for the post-monsoonal period (values higher than 1); and (c) surface without change (*i.e.,* those pixels that remains constant between the two seasons, with values around 1). In general, seasonal changes in surface MA response can be influenced by changes in terrain roughness or soil moisture content. In N. Gujarat, those changes in surface reflectivity are highly affected by the type of seasonal land use (*i.e.,* cultivation, ploughing or resting wastelands) and runoff processes that greatly affects the seasonal extension of wetlands.

3.5. Georeferencing of Subsets of Interest

The final maps were georeferenced to ground coordinates (UTM WGS94, 42N) using the ENVI function image to map registration, which requires a set of Ground Control Points (GCP). This method was preferred rather than other available geocoding methods [39,57], requiring the use of a DEM to orthorectify the imagery. However, the flat topography characterizing the dune and interdune fields limit the possibility of using DEMs as available datasets (SRTM v4 or ASTER GDEM v2) proved to be too coarse for this purpose [14].
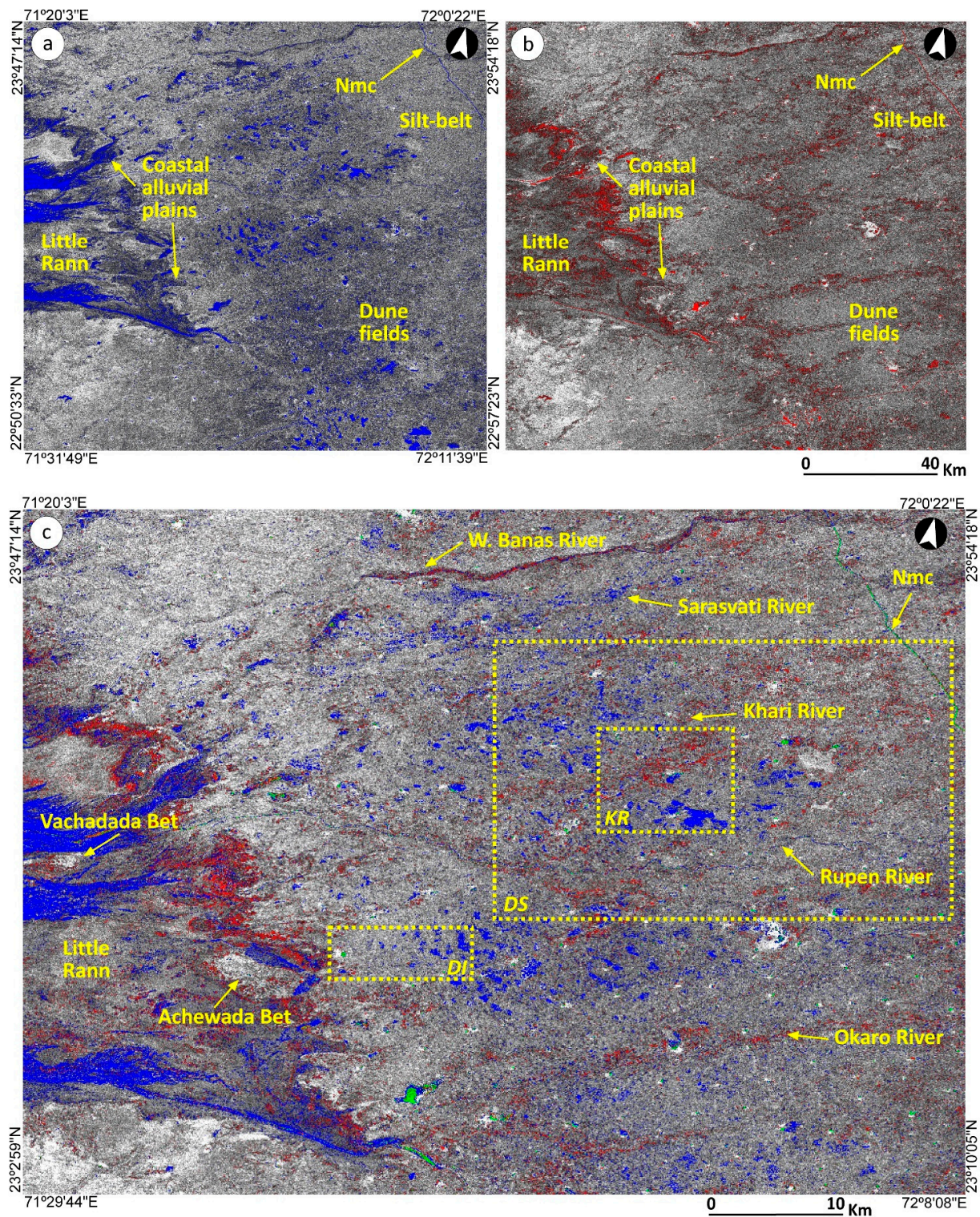
4. Results: Regional and Local Observations of Hydrological Dynamics

At the regional scale, the above-mentioned amplitude products helped to delineate three major geomorphological features in the study area. These are (a) the low-lying marsh area of the LRK and its islands (which are locally called as "bets"); (b) the coastal alluvial plains; and (c) the main rivers and watersheds that flow NE-SW towards the LRK (Figure 6).

At the local scale, results are presented in three subsets of interest within the study area to better evaluate the amplitude response in different archaeological and geomorphological settings (see dotted areas in Figure 6c):

1. Khari River (KR): This area integrates the Khari River basin area (a left bank tributary of the Rupen River) and is characterised by the presence of well-preserved dome dunes. This area has been largely explored in consecutive archaeological missions and contains several archaeological sites and scatters of dispersed materials.
2. Dune and interdune fields (DI): coastal area with fossilized dunes near Zinzuwada village. Despite the well-preserved linear dunes and fertile interdunes, to date no archaeological evidence has been found in this area.
3. Dune fields/Silt-belt (DS): This subset includes the lower Silt-belt alluvial plains (between the Narmada main canal and the WCBMF boundary) and the dune and interdune fields located between the eastern banks of the Saraswati River and the western banks of the Rupen River.

Figure 6. (**a**) Monsoonal flooding map (enhanced in blue) superimposed to monsoonal MA and (**b**) post-monsoonal flooding map (enhanced in red) superimposed to post-monsoonal MA; (**c**) Integrated seasonal flooding map. Pixels flooded on both seasons are represented in green. Dotted areas indicate the subsets of interest displayed in Figure 7 (KR), Figure 8 (DI) and Figure 9c (DS).

4.1. Little Rann of Kachchh

The maximum extent of the flood covering the LRK during the rainy season is clearly visible in Figure 6c (enhanced in blue). The mean elevation of the LRK surface is ~6 m a.s.l, which gradually decreases to 2 m towards the south-western basins [24]. This gently, regional slope drives the monsoonal spill and the post-monsoonal run-off from the coastal alluvial fans to the ocean. Although the LRK progressively dries up after the monsoonal rains, some flooded areas are still detected in Figure 6c during the post-monsoonal season (enhanced in red). Some remains of post-monsoonal water bodies can be related to stagnant water or contemporary intensive saltpan exploitation in parcels that capture monsoonal run-off. Islands (see Vachadada Bet and Achewada Bet in Figure 6c) and elevated plateaus can also be identified in both periods due to the roughness of its dry surfaces (with presence of abundant shrub vegetation). During the dry period, some small water bodies arise in the islands, suggesting a post-monsoonal use and maintenance of island ponds and water reservoirs.

It is worth noting that Figure 6b,c show a significant post-monsoonal increase of humid surfaces along the wastelands located in the coastal alluvial plains. The predominance of post-monsoonal pixels in these areas can be related to the intensification of irrigated crop fields and illegal salt panning documented by Prasad *et al.* [60] along the Wild Ass Sanctuary (*i.e.*, a protected biosphere reserve that encompasses the LRK and its coastal ecosystems). These land-use changes are critically affecting the habitat management of the Asiatic wild ass and endangered species such as Dalmatian pelican and lesser flamingo.

4.2. River Catchment Areas

The integrated seasonal flooding map in Figure 6c shows a wider and more visible monsoonal river flow within the dune and interdune fields, which corresponds to the alluvial plains that extend below the 40 m a.s.l. contour line. In the Silt-belt plains, in contrast, the riverbeds become narrower (*i.e.*, more incised). The West Banas River shows a low monsoonal flow, mainly concentrated in abundant pools and relict meandering channels, which are occasionally reactivated during the rainy season [14]. However, flooding events during high rainfall years can have high destructive impact [61]. The Rupen, Saraswati and Khari rivers have a more incised and narrow channel bed.
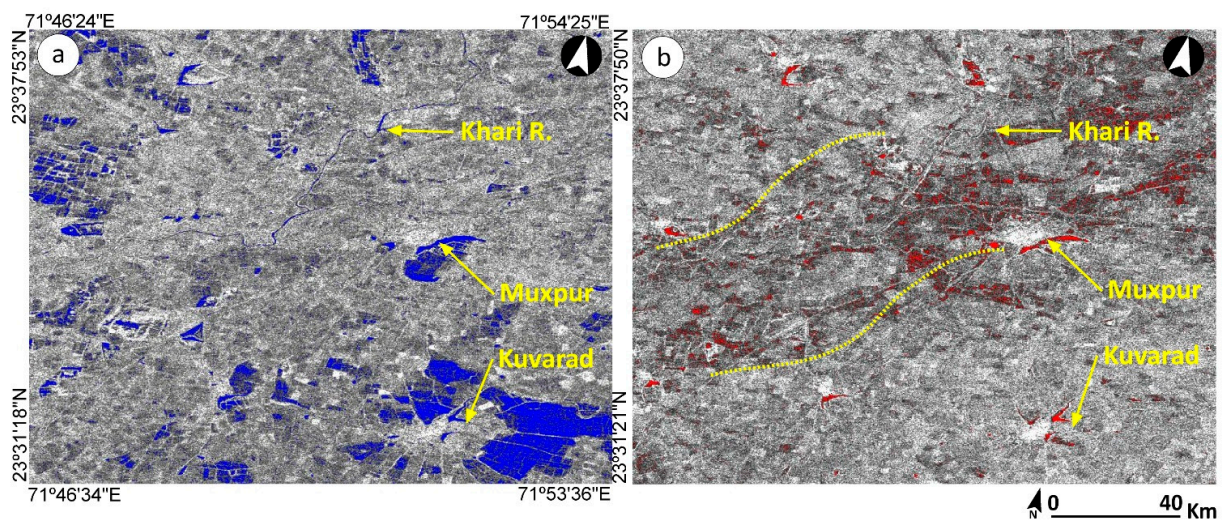
During the post-monsoonal months the detected water surfaces migrates from the dried-up riverbed towards the riverbanks and adjacent fields. Figure 7b shows post-monsoonal lower amplitude response (as suggested by the abundance of black and very dark tones) within the river catchment area, thus revealing the presence of some waterlogged areas and generally suggesting high soil moisture rates.

4.3. Village Tanks and Lakes

Village tanks and lakes have the best water harvesting performance. They reach maximum extension at the end of the monsoon and maintain water throughout the post-monsoon season (for a water tank comparison, see the tanks analyzed in Figure 5 and the seasonal flooding maps in Figure 7). In contrast, adjacent flooded interdune fields dry up shortly after the monsoon. High MA values (very bright clusters of pixels) are representative of village areas and indicate the presence of permanent and quasi-permanent water tanks with the settlements. The occurrence of quasi-permanent water bodies

correlates rather well with the distribution of villages and urban settlements (traditionally located on the top of large and prominent fossilized dunes). The original water bodies were extended in historical times and were regularly maintained to provide ecological services and much-needed water during the year. In the last years, several hydrological projects have promoted the cleaning and restoration of water tanks and temporal ponds as a way to develop sustainable water harvesting strategies [62].

Figure 7. Khari River (KR) subset of interest showing the flooding maps for (**a**) MA monsoonal (blue pixels) and (**b**) MA post-monsoonal images (red pixels). Note the post-monsoonal low amplitude (dark pixels) in the field banks located within the Khari River basin area (yellow dotted line).
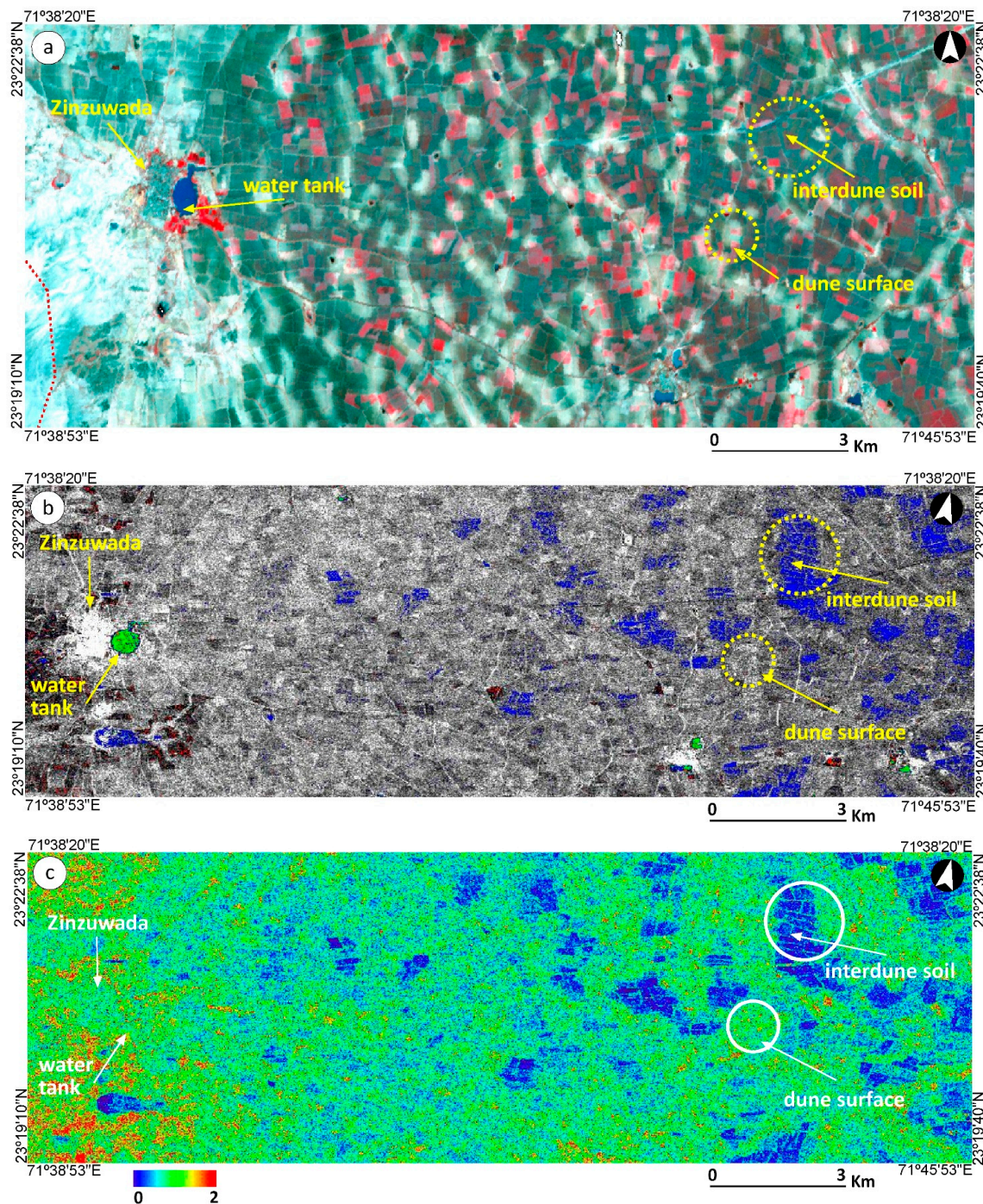

4.4. Interdune Waterlogging

Amplitude values reveal, as expected, significant changes between the two observed seasons in interdune waterlogging and water run-off (Figure 8). Interdune soils are dark coloured vertisols rich in clay and humus, locally known as black cotton soils and they are characterized by colluvium fine sediments (*i.e.*, clay) and rich organic content. In post-monsoonal multispectral false color imagery, the interdune surface is generally represented by dark green tones (Figure 8a). Clay soils have little water percolation but fast saturation rates, falling into cracks in dry periods [63]. The integrated seasonal flooding map in Figure 8b reveals significant flooding pixels in interdune fields during the monsoon, which suggest the presence of quick-lived water bodies with fast evotransporation and loss of water content. Very low darkish amplitude in other fields may suggest abundant soil moisture but no water logging. Check dams and temporal ponds distributed in the dune-interdune sector of the study area retain water for short periods, depending of the intensity of rainfall.

Figure 8c displays the MA ratio between monsoonal and post-monsoonal MA values. A good correlation between values with small season variability can be related to permanent anthropic features in the landscape (*i.e.*, Zinzawada village and its water tank). On the other hand, the ratio of interdune fields reflects flood-prone areas that could retain soil moisture during the post-monsoonal period, whereas MA change values for fossilized dunes indicates a surface stability (*i.e.*, non-floodable areas) between seasons.

Figure 8. (**a**) Dune-interdune (DI) subset of interest in orthorectified ASTER false colour composite (3N-2-1) from 1 October 2004; (**b**) Integrated seasonal flooding map (blue for monsoon, red for post-monsoon and green for no change); (**c**) Seasonal MA change values (stretched histogram).

5. Discussion

5.1. Tectonic Influence and Modern Disturbances

Land use change, the construction of dams in the 60s and the presence of large irrigation canals has substantially altered the nature and frequency of flooding discharge and run-off in N. Gujarat.

In addition, observed changes in the water flow and the high variability of seasonal water-bodies might be also a partial result of post-monsoonal tube-well irrigation, which is a well-distributed activity hard to detect by the medium resolution provided by C-band imagery.

The Narmada main canal is the major hydrological infrastructure in the study area. Its size makes it visible in amplitude images (e.g., in Figure 6 where the green pixels indicate constant water flow in the canal through the year). The canal brings water into the study area from the catchments of the southern river basins. However, while the main canal started to function in the early 2000s, the secondary branches that serve the study area were only fully activated in 2010 [35–38]. Therefore, we can reasonably assume that the Narmada canal had virtually no effect on the natural available water capacity of our study area between 2004 and 2009, *i.e.*, during our time window observation.

Notwithstanding, the major factors involved in N. Gujarat hydrological patterns for the period of observation are related to tectonic influence and regional altimetry. The alluvial Quaternary deposition within the depression of the Cambay basin (*i.e.*, Silt-belt) set in place deeper unsaturated aquifers that allow (1) more rainfall infiltration into the soil surface and (2) faster water table recharge. In contrast, the more permeable inter-dune silts retain monsoonal moisture, whereas interdune fields located within river basin areas experience major infiltration rates and water run-off towards the Little Ran.

Overall, the following patterns emerge:

1. In the Silt-belt, unconfined aquifers and permeable silty soils favour water infiltration and water table recharge, reducing run-off and increasing soil pedogenesis.
2. In the dune/interdune fields, rain falling on impermeable saturated soils runs off.
3. River basins act as ecological corridors between the two areas, with presence of humid soils along the watersheds independently of the surrounding context.

5.2. Implications for Archaeology

The above observations of regional and local hydrological dynamics have provided a framework for evaluating present-day and historical trajectories of both natural and anthropic monsoonal patterns as well as the use and distribution of water resources. As a tool to evaluate these trajectories, the georeferenced SAR derived maps provided a new and robust means to examine the distribution patterns of the NoGAP archaeological data in the context of the amplitude signatures for the ISM rainfall. As noted above, paleoclimatic models for the Asian monsoon [31] suggest a rather stable seasonal variability through the Holocene. Therefore, the amplitude images used in this study can be used as an explorative approach to examine long-term human occupation in the study area,

At the regional scale, the major concentrations of mid-Holocene settlements are in the dune/interdune fields located between the 8 m and 40 m a.s.l. contour lines (Figure 9a). The boundary that marks the 8 m contour line also helps to delineate the coastal alluvial plains that connect the LRK with the continental lands. The absence of surface scatters in this area could be related to taphonomical processes influenced in recent times by the increase of cultivated fields and salt panning in this area.

Figure 9. (**a**) Georeferenced seasonal flooding map (blue for monsoon, red for post-monsoon and green for no change) and regional distribution of archaeological sites; (**b**) Integrated seasonal flooding map superimposed to regional elevation (SRTM 90 v4.1, http://srtm.csi.cgiar.org); (**c**) Integrated seasonal flooding map superimposed to the MA image for the Dune fields/Silt-b*e*lt (DS) subset of interest (dotted areas indicates the extent of Figure 10a,b).
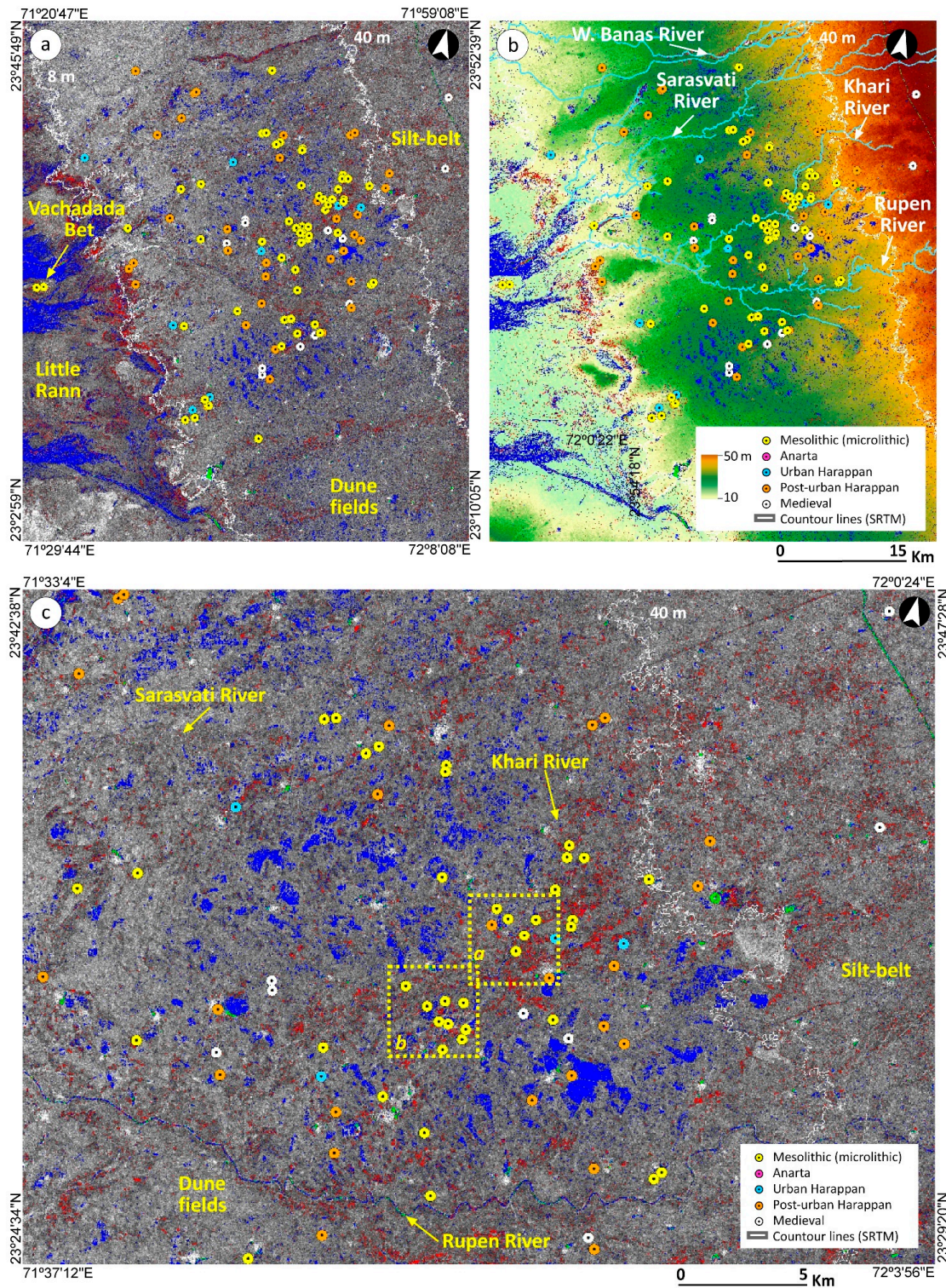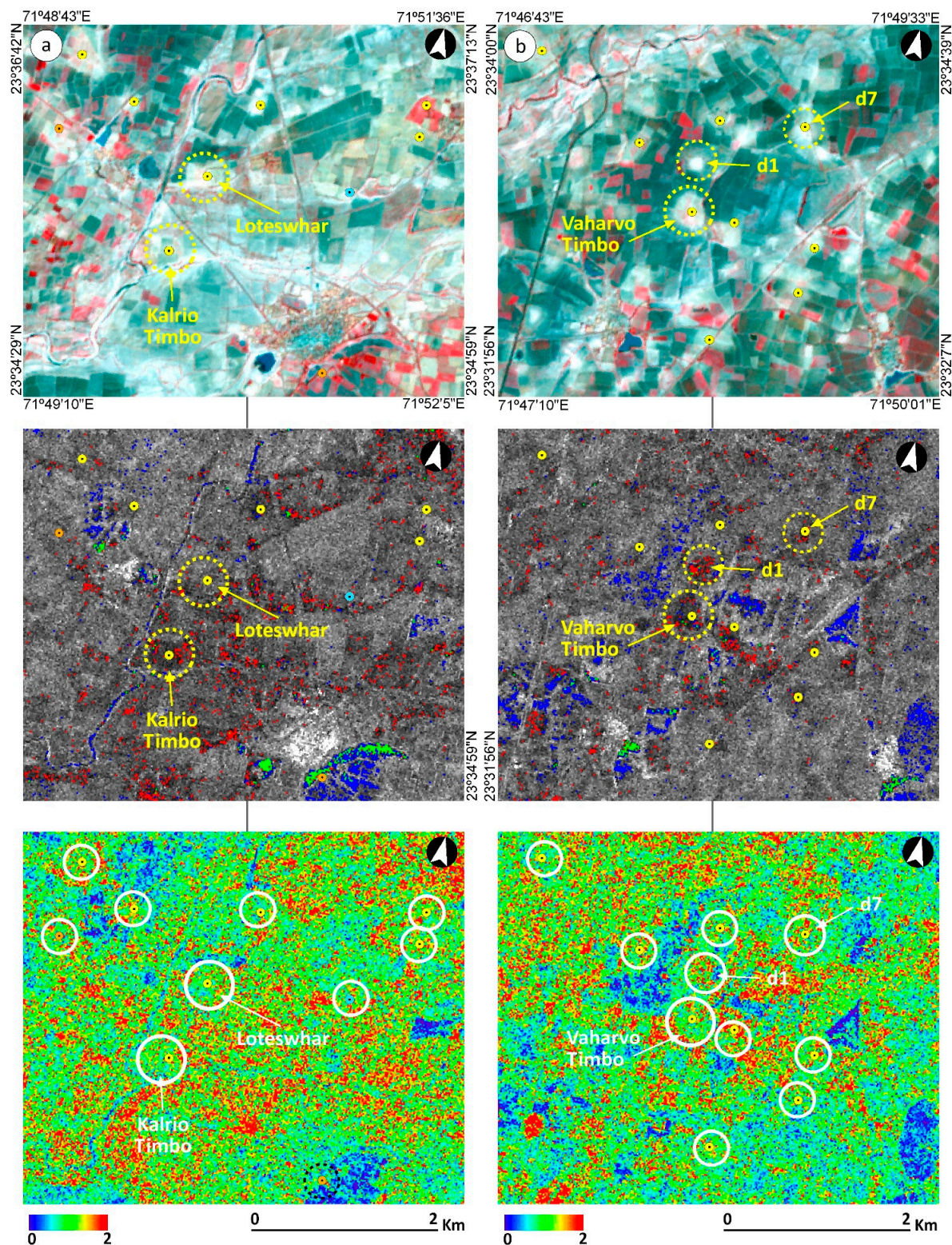
Figure 10. Subset detail of two archaeological areas within the Khari River basin area: (**a**) Loteshwar/Kalrio Timbo and (**b**) Vaharvo Timbo. Image composition shows, in descending order: orthorectified ASTER false colour composite (3N-2-1) from 1 October 2004; integrated seasonal flooding maps (blue for monsoon, red for post-monsoon and green for no change) superimposed to MA images; and seasonal MA change map (stretched histogram).

On the other hand, a major presence of Mesolithic hunter-gatherer sites (primarily represented by microlithic surface scatters) is attested within the Khari River basin. The abundance of these sites suggests a recurrent occupation of riverbanks for hunter-gatherer groups. As suggested by Bhan [16,64] the banks of the Rupen River and its tributaries have excellent growth of nutritious fodder which is available after the first monsoonal rainfall, attracting diverse types of regional fauna. This fodder is used today for enhanced milk production due to higher protein content, as attested in current ethno-archaeological studies regarding present day nomadic pastoralists [16,64].

It is possible that the river basin could have presented an attractive resource spot for past pastoral communities (represented in Figure 9 by Anarta and Harappan related communities). Some of the hunter-gatherer sites located along the Khari River show signs of repeated occupation over several millennia. For example, the excavations of the fossilized dune of Loteshwar suggests a seasonal occupation by hunter-gatherers c. 9–7.5 ka cal BP and by agro-pastoral groups c. 5.7–4.2 ka cal BP [65]. Therefore, the seasonal water availability in N. Gujarat may suggest two different strategies for seasonal campsites, taking advantage of monsoonal flooding in interdune areas but also having rich spots of soil moisture and denser vegetation along the watercourses.

Fossilized dunes are most visible in local seasonal MA change maps (Figure 10a,b) whereas values in green represent areas that remain stable between seasons, in clearly contrast with the surrounding flood-prone areas (*i.e.*, black-cotton soils and riverbanks). The higher archaeological dunes (*i.e.*, Loteshwar and Kalrio Timbo in Figure 10a and Vaharvo Timbo in Figure 10b) have the most stable amplitude as they are elevated ~5 m from the floodable interdune black-cotton soils. In contrast, less prominent dunes are prone to seasonal changes. For example, as suggested by the seasonal MA change map in Figure 10b, dune surfaces coded d1 and d7 show constant high multispectral reflectance (*i.e.*, bright tones) in both the monsoon and post-monsoon season. Conversely, the amplitude post-monsoonal flooding map shows that these dunes become flood-prone areas during the post-monsoonal period. Seasonal MA change map also suggests a high rate of variability. This pattern could be explained by the low elevation of these dunes, which facilitates cultivation and often destroys archaeological evidence. The consequent impact on archaeological visibility could explain the absence of surface materials in dune d1 and the low presence of artifacts and ecofacts in dune d7.

6. Conclusions

This work demonstrates how Synthetic Aperture Radar (SAR) C-band amplitude response in monsoonal semi-arid environments represents a step forward towards the archaeological use of satellite radar data in the context of the Greater Indus Valley (Northern India and Pakistan). ENVISAT ASAR allows the multi-temporal investigation of this area, overcoming the limitations of optical Earth Observation data related principally to heavy cloud coverage during the monsoonal period.

The amplitude seasonal flooding maps, elaborated for this work through the processing of radar images, allowed the identification of active morphogenic processes affecting pedological conditions and water distribution in the semi-arid region of North Gujarat. The alluvial plains located between the coastal marshes areas of the Little Rann of Katchchh and the Western Cambay Basin Margin Fault boundary (along the 40 m a.s.l. contour line) are characterized by well-preserved sand dunes that remain dry throughout the year, and seasonally flooded interdune areas. The main watercourses of the

study area discharge into the Little Rann and show well-defined palaeochannels and frequent avulsion episodes. Although the main discharge of these rivers happens during the onset of the Indian Summer Monsoon (June to September), amplitude response in the post-monsoonal months (October to January) suggests abundant water retention in the near-river water table. These seasonal dynamics of water discharge have most probably influenced the prehistoric and historical patterns of landscape exploitation by human groups with diverse economic strategies (hunter-gatherers, agro-pastoralists and farmers). Indeed, the integration of archaeological evidence with SAR amplitude images shows that human occupation was recurrent on raised dunes located close to areas with higher water retention, which represent potential resources hotspots through the post-monsoonal months (e.g., interdunes, lakes, and river banks).

Our observations have strong repercussions for the understanding of human occupation dynamics in the region, where a positive feedback cycle seems to have been in place for several centuries and possibly millennia. Prominent dunes, where most archaeological scatters are documented, can be identified in mean amplitude change maps as the most stable landscape feature during the entire year. This suggests a preference for recurrent seasonal camps. In addition, most of the prominent dunes are still occupied by present-day villages, or have been converted in fortified temples (e.g., Loteshwar temple, one of the earliest attested in the region). This long-term recurrence of occupation that stretches to present-day strengthens the hypothesis of the importance of prominent dunes as places of settlement in this area. In addition, the use of mean amplitude change maps allows the identification of land-cover changes (e.g., irrigation activities such as tube well irrigation and construction of canals) on fossilized dune surfaces that jeopardize archaeological preservation and visibility.

Further research is needed to understand the hydrological dynamics during the dry season and to confirm the observed patterns on the ground. In light of this, a geoarchaeological survey was carried out across the study area and a set of surface sediment samples were collected from several geomorphological features (mostly dunes, interdune soils and riverbeds) during the post-monsoonal months. The on-going physical characterization of these soils will provide more data to direct further SAR approaches. In addition, we have acquired new high-resolution SAR imagery (TerraSAR-X Single-Look StripMap and SpotLight imagery). These new acquisitions will improve the quality of our data and expand our temporal window to include the impact on archaeological preservation of more recent irrigation works.

Acknowledgements

Author Contributions

Francesc C. Conesa and Núria Devanthéry conceived and designed the research and performed the analyses; Francesc C. Conesa, Núria Devanthéry, Andrea L. Balbo, Marco Madella and Oriol Monserrat analyzed the data; Francesc C. Conesa, Núria Devanthéry, Andrea L. Balbo and Marco Madella wrote the paper.

Conflicts of Interest

The authors declare no conflict of interest.

References

1. Agrawal, D.P.; Pande, B.M. *Ecology and Archaeology of Western India*; Naurang Rai: Anand Nagar, India, 1977.
2. Allchin, R.; Allchin, B. Pathways to settled life: The Mesolithic and early Neolithic. In *The Rise of Civilization in India and Pakistan*; Cambridge University Press: Cambridge, UK, 1982.
3. Fuller, D.Q.; Madella, M. Issues in Harappan archaeology: Retrospect and prospect. In *Protohistory: Archaeology of the Harappa Civilization*; Settar, R., Korisettar, R., Eds.; Manohar: Delhi, India, 2002; pp. 317–390.
4. Madella, M.; Fuller, D.Q. Palaeoecology and the Harappan civilisation of South Asia: A reconsideration. *Quat. Sci. Rev.* **2006**, *25*, 1283–1301.
5. Farooqui, A.; Gaur, A.S.; Prasad, V. Climate, vegetation and ecology during Harappan period: Excavations at Kanjetar and Kaj, mid-Saurashtra coast, Gujarat. *J. Archaeol. Sci.* **2013**, *40*, 2631–2647.
6. Thomas, K.D. Minimizing risk? Approaches to pre-Harappan human ecology on the north-west margin of the Greater Indus system. In *Indus Ethnobiology: New Perspectives from the Field*; Weber, S.A., Belcher, W.R., Eds.; Lexington Books: Lanham, MD, USA, 2003; pp. 397–430.
7. Meadow, R. The origins and spread of agriculture and pastoralism in northwestern South Asia. In *The Origins and Spread of Agriculture and Pastoralism in Eurasia*; Harris, D.R., Ed.; UCL Press: London, UK, 1996; pp. 390–412.
8. Khadkikar, A.S.; Mathew, G.; Malik, J.N.; Gundu Rao, T.K.; Chowgaonkar, M.P.; Merh, S.S. The influence of the south-west Indian monsoon on continental deposition over the past 130 kyr, Gujarat, western India. *Terra Nova* **1999**, *11*, 273–277.
9. Chamyal, L.S.; Maurya, D.M.; Raj, R. Fluvial systems of the drylands of western India: A synthesis of Late Quaternary environmental and tectonic changes. *Quat. Int.* **2003**, *104*, 69–86.

10. Sharma, C.S.; Behera, M.D.; Mishra, A.; Panda, S.N. Assessing flood induced land-cover changes using remote sensing and fuzzy approach in Eastern Gujarat (India). *Water Resour. Manag.* **2011**, *25*, 3219–3246.

11. Ajithprasad, P. Holocene adaptations of the Mesolithic and Chalcolithic settlements in north Gujarat. In *Monsoon and Civilizations*; Yasuda, Y., Shinde, V., Eds.; Roli Books: New Delhi, India, 2004; pp. 115–132.

12. Ajithprasad, P. Chalcolithic cultural patterns and the early Harappan interaction in Gujarat. In *Cultural Relations between the Indus and the Iranian Plateau During the Third Millenium BCE*; Osada, T., Witzel, M., Eds.; Harvard Oriental Series: Cambridge, UK, 2011; pp. 11–42.

13. Rajesh, S.V.; Krishnan, K. Chalcolithic cultures of Gujarat (c. 3950–900 BCE): An aappraisal. In *Pracyabodha. Indian Archaeology and Tradition*; Mani, B.R., Singhvi, A.K., Kumar, R., Eds.; B.R. Publishing Corporation: New Delhi, India, 2014; pp. 194–205.

14. Balbo, A.L.; Rondelli, B.; Cecília Conesa, F.; Lancelotti, C.; Madella, M.; Ajithprasad, P.; Conesa, F.C. Contributions of geoarchaeology and remote sensing to the study of Holocene hunter–gatherer and agro-pastoral groups in arid margins: The case of North Gujarat (Northwest India). *Quat. Int.* **2013**, *308–309*, 53–65.

15. Rajesh, S.V.; Krishnan, K.; Ajithprasad, P.; Sonawane, V.H. Evaluating the Anarta tradition in the light of Material culture from Loteshwar and other sites in Gujarat. *Man Environ.* **2013**, *38*, 10–45.

16. Bhan, K.K. Pastoralism in Late Harappan Gujarat, western India: An ethnoarchaeological approach. In *Linguistics, Archaeology and the Human Past*; Osada, T., Uesugi, A., Eds.; Research Institute for Humanity and Nature: Kyoto, Japan, 2011; pp. 1–27.

17. Ajithprasad, P.; Sonawane, V.H. The Harappa culture in North Gujarat: A regional paradigm. In *Linguistics, Archaeology and the Human Past*; Osada, T., Uesugi, A., Eds.; Research Institute for Humanity and Nature: Kyoto, Japan, 2011; pp. 223–269.

18. Sonawane, V.H. Early farming communities of Gujarat, India. *Indo-Pac. Prehist. Assoc. Bull.* **2000**, *19*, 137–146.

19. Madella, M.; Ajithprasad, P.; Lancelotti, C.; Rondelli, B.; Balbo, A.L.; French, C.A.I.; Rodríguez, D.; García-Granero, J.J.; Yannito, V.; Rajesh, S.V.; *et al.* Social and environmental transitions in arid zones: The North Gujarat Archaeological Project—NoGAP. *Antiq. Proj. Gallery* **2010**, *84*, 1–4.

20. Lancelotti, C.; Caracuta, V.; Fiorentino, G.; Madella, M.; Ajithprasad, P. Holocene monsoon dynamics and human occupation in Gujarat: Stable isotopes analyses on plant remains. *J. Multidiscip. Stud. Archaeol.* **2013**, *1*, 288–300.

21. Madella, M.; Rondelli, B.; Lancelotti, C.; Balbo, A.; Zurro, D.; Campillo, X.R.; Stride, S. Introduction to simulating the past. *J. Archaeol. Method Theory* **2014**, doi:10.1007/s10816-014-9209-8.

22. Conesa, F.C.; Madella, M.; Galiatsatos, N.; Balbo, A.L.; Rajesh S.V.; Ajithprasad, P. CORONA photographs in monsoonal semi-arid environments: Addressing archaeological surveys and historic landscape dynamics over north Gujarat, India. *Archaeol. Prospect.* **2014**, doi:10.1002/arp.1498.

23. Balbo, A.L.; Rubio-Campillo, X.; Rondelli, B.; Ramírez, M.; Lancelotti, C.; Torrano, A.; Salpeteur, M.; Lipovetzky, N.; Reyes-García, V.; Montañola, C.; *et al.* Agent-based simulation of Holocene Monsoon precipitation patterns and hunter-gatherer population dynamics in semi-arid environments. *J. Archaeol. Method Theory* **2014**, *21*, 426–446.

24. Maurya, D.M.; Thakkar, M.G.; Khonde, N.; Chamyal, L.S. Geomorphology of the Little Rann of Kachchh, W. India: Implication for basin architecture and Holocene palaeo-oceanographic conditions. *Z. Für Geomorphol.* **2009**, *53*, 69–80.

25. Juyal, N.; Chamyal, L.S.; Bhandari, S.; Bhushan, R.; Singhvi, A.K. Continental record of the southwest monsoon during the last 130 ka: Evidence from the southern margin of the Thar Desert, India. *Quat. Sci. Rev.* **2006**, *25*, 2632–2650.

26. Srivastava, P.; Juyal, N.; Singhvi, A.K.; Wasson, R.J.; Bateman, M.D. Luminescence chronology of river adjustment and incision of Quaternary sediments in the alluvial plain of the Sabarmati River, north Gujarat, India. *Geomorphology* **2001**, *36*, 217–229.

27. Juyal, N.; Kar, A.; Rajaguru, S.N.N.; Singhvi, A.K. Luminescence chronology of aeolian deposition during the Late Quaternary on the southern margin of Thar Desert, India. *Quat. Int.* **2003**, *104*, 87–98.

28. Attri, S.D.; Tyagi, A. *Climate profile of India*; India Meteorological Department: New Delhi, India, 2010.

29. Singhvi, A.K.; Williams, M.J.; Rajaguru, S.N.; Misra, V.N.; Chawla, S.; Stokes, S.; Chauhan, N.; Francis, T.; Ganjoo, R.K.; Humphreys, G.S. A 200 ka record of climatic change and dune activity in the Thar Desert, India. *Quat. Sci. Rev.* **2010**, *29*, 3095–3105.

30. Sareen, B.K.; Tandon, S.K.; Bhola, A.M. Slope-deviatory alignment, stream network and lineament orientation of the Sabarmati River system-Neotect. *Curr. Sci.* **1993**, *64*, 827–836.

31. Liu, Z.; Otto-Bliesner, B.; Kutzbach, J.; Li, L.; Shields, S. Coupled climate simulation of the evolution of global monsoons in the Holocene. *J. Clim.* **2003**, *16*, 2472–2490.

32. McIntosh, J.R. *The Ancient Indus Valley: New Perspectives*; ABC-CLIO: Santa Barbara, CA, USA, 2008.

33. Dixit, A.K. Agriculture in a high growth state: Case of Gujarat (1960 to 2006). *Econ. Polit. Wkly.* **2009**, *69*, 64–71.

34. Fishman, R.; Jain, M.; Kishore, A. *Patterns of Migration, Water Scarcity and Caste in Rural Northern Gujarat*; International Growth Centre: London, UK, 2013.

35. Ranade, R.; Kumar, M.D.; Management, C.; Projects, L.I. Narmada water for groundwater recharge in north Gujarat. *Econ. Political Wkly.* **2004**, *39*, 3510–3513.

36. Kumar, M.D.; Singhal, L.; Rath, P. Value of groundwater: Case studies in Banaskantha. *Econ. Political Wkly.* **2004**, *39*, 3498–3503.

37. Shah, T.; Bhatt, S.; Shah, R.K.; Talati, J. Groundwater governance through electricity supply management: Assessing an innovative intervention in Gujarat, western India. *Agric. Water Manag.* **2008**, *95*, 1233–1242.

38. Narula, K.; Fishman, R.; Modi, V.; Polycarpou, L. *Addressing the Water Crisis in Gujarat, India*; Columbia Water Center: New York, NY, USA, 2011.

39. Holcomb, D.W.; Shingiray, I. Imaging radar in archaeological investigations: An image processing perspective. In *Remote Sensing in Archaeology*; Wiseman, J., El-Baz, F., Eds.; Springer: New York, NY, USA, 2007; pp. 11–46.

40. Hall, O. Remote sensing in social science research. *Open Remote Sens. J.* **2010**, *3*, 1–16.

41. Lasaponara, R.; Masini, N.; Observation, E. Satellite remote sensing in archaeology: Past, present and future perspectives. *J. Archaeol. Sci.* **2011**, *38*, 1995–2002.

42. Comer, D.C.; Harrower, M.J. *Mapping Archaeological Landscapes from Space*; Springer: New York, NY, USA, 2013; pp. 291–313.

43. Lasaponara, R.; Masini, N. Satellite synthetic aperture radar in archaeology and cultural landscape: An overview. *Archaeol. Prospect.* **2013**, *20*, 71–78.

44. Oberstadler, R.; Hönsch, H.; Huth, D. Assessment of the mapping capabilities of ERS-1 SAR data for flood mapping: A case study in Germany. *Hydrol. Process.* **1997**, *11*, 1415–1425.

45. Martinez, J.M.; Le Toan, T. Mapping of flood dynamics and spatial distribution of vegetation in the Amazon floodplain using multitemporal SAR data. *Remote Sens. Environ.* **2007**, *108*, 209–223.

46. Khan, S.; Hong, Y.; Gourley, J.; Khattak, M.; De Groeve, T. Multi-sensor imaging and space-ground cross-validation for 2010 flood along Indus River, Pakistan. *Remote Sens.* **2014**, *6*, 2393–2407.

47. Grady, D.O.; Leblanc, M.; Gillieson, D.; O'Grady, D. Use of ENVISAT ASAR Global Monitoring Mode to complement optical data in the mapping of rapid broad-scale flooding in Pakistan. *Hydrol. Earth Syst. Sci.* **2011**, *15*, 3475–3494.

48. Park, N.; Patel, P.; Srivastava, H.S.; Navalgund, R.R. Use of synthetic aperture radar polarimetry to characterize wetland targets of Keoladeo National Park, Bharatpur, India. *Curr. Sci.* **2009**, *97*, 529–537.

49. Rajawat, A.S., Verma, P.K., Nayak, S.; Rajawat, A.S.; Verma, P.K.; Nayak, S. Reconstruction of paleodrainage network in northwest India: Retrospect and prospects of remote sensing based studes. *Proc. Indian Natn. Sci. Acad.* **2003**, *69*, 217–236.

50. Pirasteh, S.; Rizvi, S.M.A.; Ayazi, M.H.; Safari, H.; Ramli, F.M.; Pradhan, B.; Shattri, M.; Mahmoodzadeh, A.; Pirateh, S.; Rizvi, S.M.A.; *et al.* Using ERS-1 synthetic aperture radar for flood delineation, Bhuj Taluk, Kuchch District-Gujarat, India. *Int. Geoinform. Res. Dev. J.* **2010**, *1*, 13–22.

51. Rajawat, A.S.; Kumar, R.; Murthy, T.V.R.; Haldar, D.; Chakraborty, A.; Kumar, T.; Sneha, R.; Kumar, H.; Mahapatra, M.; Kundu, S. Initial results using RISAT-1 C-band SAR data. *Curr. Sci.* **2013**, *104*, 490–501.

52. Thakker, P.S.; Bhatnagar, G.C.; Rao, M.K.; Raval, M.H. Mapping of palaeo- channels along the river Sabarmati and Banas in Gujarat using Landsat data. In *Remote Sensing and Archaeology*; Tripathy, A., Ed.; Sundeep Prakashan: New Delhi, India, 2005; pp. 169–175.

53. Rajani, M.B.; Rajawat, A.S. Potential of satellite based sensors for studying distribution of archaeological sites along palaeo channels: Harappan sites a case study. *J. Archaeol. Sci.* **2011**, *38*, 2010–2016.

54. Wright, R.; Hritz, C. Satellite remoe sensing imagery: New evidence for site distributions in the upper Indus. In *South Asian Archaeology 2007. Prehistoric Periods*; Frenez, D., Tosi, M., Eds.; Archaeopress: Oxford, UK, 2013; pp. 315–321.

55. Sinha, R.; Yadav, G.S.; Gupta, S.; Singh, A.; Lahiri, S.K. Geo-electric resistivity evidence for subsurface palaeochannel systems adjacent to Harappan sites in northwest India. *Quat. Int.* **2013**, *308–309*, 66–75.

56. Tapete, D.; Cigna, F.; Masini, N; Lasaponara, R. Prospection and monitoring of the archaeological heritage of Nasca, Peru, with ENVISAT ASAR. *Archaeol. Prospect.* **2013**, *20*, 133–147.

57. Cigna, F.; Tapete, D.; Lasaponara, R.; Masini, N. Amplitude change detection with ENVISAT ASAR to image the cultural landscape of the Nasca region, Peru. *Archaeol. Prospect.* **2013**, *20*, 117–131.

58. Bartsch, A.; Doubkova, M.; Pathe, C.; Sabel, D.; Wagner, W.; Wolski, P. River flow & wetland monitoring with ENVISAT ASAR Global Mode in the Okavango basin and delta. In Proceedings of the Second IASTED Africa Conference Water Resource Management, Gabarone, Botswana, 8–10 September 2008; pp. 152–156.

59. Khan, K.A.; Akhter, G.; Ahmad, Z. Integrated geoscience databanks for interactive analysis and visualization. *Int. J. Digit. Earth* **2011**, *6*, 41–49.

60. Prasad, S.N.; Goyal, S.P.; Rov, P.S.; Singh, S. Changes in wild ass (Equus hemionus khur) habitat conditions in Little Rann of Kutch, Gujarat from a remote sensing perspective. *Int. J. Remote Sens.* **1994**, *15*, 3155–3164.

61. Sethi, A. *Gujarat: National Disaster Risk Reduction Portal*; National Institute of Disaster Management: New Delhi, India, 2014.

62. Agarwal, A.; Narain, S. Making water management everybody's business: Water harvesting and rural development in India. *Gatekeep. Ser.* **1999**, *87*, 3–20.

63. Babu, P.V. Geomorphology if the cambay basin. *J. Indian Soc. Photo-Interpret.* **1977**, *5*, 9–17.

64. Bhan, K.K. Cultural development of the prehistoric period in north Gujarat with reference to western India. *South Asian Stud.* **1994**, *10*, 71–90.

65. Patel, A.K. Occupational histories, settlements, and subsistence in western India: What bones and genes can tell us about the origins and spread of Pastoralism. *Anthropozoologica* **2009**, *44*, 173–188.